Doping Level Change of Polyaniline Film During Its Electrochemical Growth Process

Chen Liu, Jiaxin Zhang, Gaoquan Shi, Feng'en Chen

Department of Chemistry, Tsinghua University, Beijing 100084, People's Republic of China

Received 24 Feburary 2003; accepted 5 September 2003

ABSTRACT: Polyaniline (PANI) films doped with hydrochloric acid have been electrochemically deposited on mirrorlike platinum electrode surfaces by a cyclic voltammogram method. The Raman spectra of doped PANI films were investigated by excitation with a 633- or 785-nm laser beam. It was found that the overall features of the Raman spectra depend strongly on the film thickness, due mainly to that the doping level of PANI film increases during the film-growth process. X-ray photoelectron spectroscopic (XPS) analysis and ultraviolet (UV)-visible absorption spectrum results also confirmed this finding. © 2004 Wiley Periodicals, Inc. J Appl Polym Sci 92: 171–177, 2004

Key words: polyaniline; Raman spectroscopy; structure

INTRODUCTION

Polyaniline (PANI) is one of the most important conducting polymers, due to its potential applications in secondary batteries, electrochromic displays, and nonlinear microelectronic devices.[1–5] It has always considered to be an unusual class of a conducting polymer, because it differs from other conducting polymers by incorporation of a nitrogen atom between phenyl rings. Usually, PANI films can be obtained by electrochemical synthesis, while powders are produced by chemical polymerization. However, many characteristics of PANI depend strongly on synthesis techniques and experimental conditions.

Raman spectroscopy has been proved to be a useful method for studying the structure, especially the doping and dedoping process, of conducting polymers. Using Raman spectroscopy and other techniques, our previous research discovered that the doping level of many conducting polymer films, including polythiophene[6,7] and polypyrrole,[8] increases during the film-growth process. In this article, we report on a similar phenomenon on PANI films electrochemically deposited on a smooth platinum electrode. X-ray photoelectron spectroscopic (XPS) analysis and ultraviolet (UV)-visible absorption spectral results also confirmed this finding.

Correspondence to: G. Shi (gshi@tsinghua.edu.cn).

Contract grant sponsor: National Natural Science Foundation of China; contract grant numbers: 50133010; 10374034; 50225311.

Journal of Applied Polymer Science, Vol. 92, 171–177 (2004)

EXPERIMENTAL

Aniline was purchased from the Beijing Changping Shiying Chemical Engineering Plant of China (Beijing, China) and used after purification. The purification steps were as follows: First, it was distilled at 182°C and then refluxed with iron powder for 1 h. Finally, it was distilled decompressly under a nitrogen environment after drying by sodium hydroxide for 12 h.[9]

Electrochemical syntheses and examinations were performed in a one-compartment cell using a Model 283 potentiostat–galvanostat (EG&G Princeton Applied Research) under computer control. The working and counter electrodes were platinum sheets with a surface area of 0.5 cm^2 each and placed 0.5 cm apart. In the UV-visible absorption spectroscopic examinations, the working electrode was replaced by an indium tin oxide (ITO)-coated glass sheet. The surfaces of the electrodes were shiny and flat and cleaned ultrasonically after each synthesis. All potentials were referred to a saturated calomel electrode (SCE) immersed in the solution. The electrolyte solution was an aqueous solution of 1 mol L^{-1} HCl + 0.5 mol L^{-1} aniline. All solutions were deaerated by a dry nitrogen stream and maintained under a slight nitrogen overpressure during the experiments. PANI doped with HCl was deposited uniformly on the working electrode surfaces voltammetrically in the potential scale between −0.2 and +0.75 V (versus SCE) with scan rate of 0.02 V s^{-1}.

Raman spectra were carried out using an RM 2000 microscopic confocal Raman spectrometer (Renishaw PLC, England) employing a 633- or 785-nm laser beam and a CCD detector with a 4-cm^{-1} resolution. The PANI films coated on the electrode surfaces were washed with deionized water for several times to remove the electrolyte and monomer and finally air-

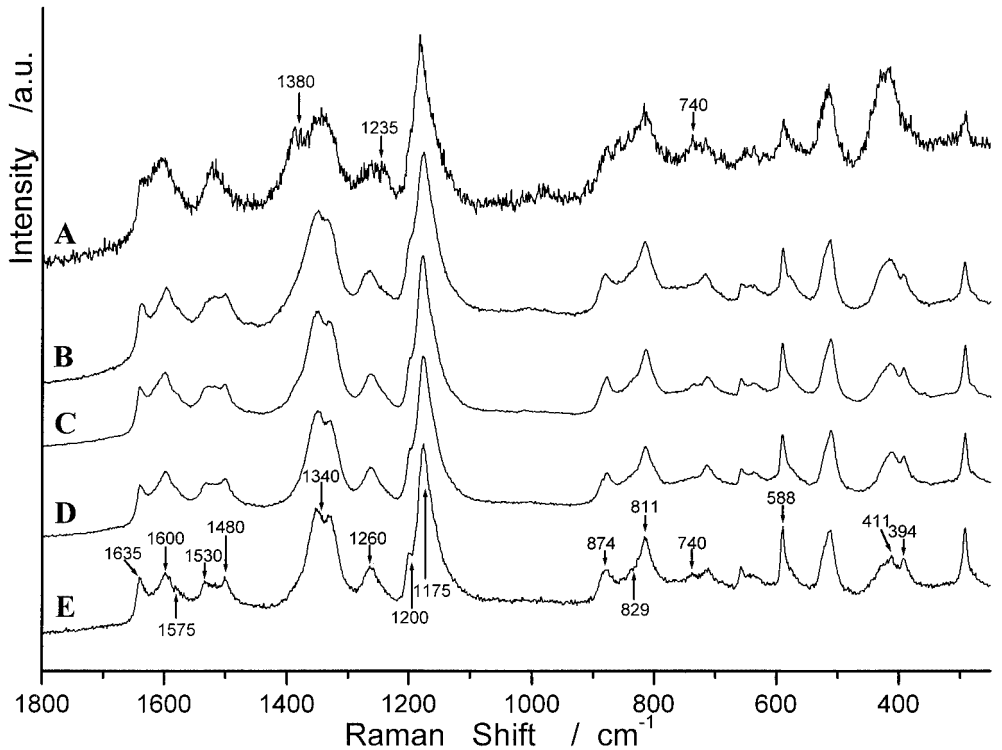

Figure 1 Excited Raman spectra, 785 nm, of PANI films deposited on Pt electrodes prepared by voltammetic scanning for different cycles in the potential scale between −0.2 and +0.75V (versus SCE) at a potential scan rate of 0.02 V s^{-1}: (A) 30 cycles; (B) 50 cycles; (C) 80 cycles; (D) 100 cycles; (E) 120 cycles.

dried for several minutes before Raman characterizations. To avoid SERS effects, the electrodes with shiny and slick surfaces were used. Scanning electron micrograph (SEM) pictures indicated that they had smooth and regular surface morphologies. The spectra were recorded by focusing a 1–2 μm laser spot on the surface of the polymer films using a 20× objective and accumulated for three times and 30 s each. The power was always kept very low (~0.1 mW) to avoid destruction of the samples. Some complex Raman peaks are divided into component Lorentzian or Gauss peaks with proper background subtraction using "automatic fitting" programs provided by the Raman spectrometer.

SEMs were taken using a KYKY 2800 electron micrographer (Scientific Instrumental Plant of Chinese Academy of Science), and the thickness of the PANI films was read from the SEM graphs. XPS examinations were performed by the use of an AEM PHI5300 spectrometer of the PE Co. UV-visible absorption spectroscopic examinations were carried out on an Ultra-spec 4000 spectrometer of the Bio-tech Co.

RESULTS AND DISCUSSION

The 785- and 633-nm laser-excited Raman spectra of PANI films with different thicknesses are shown in Figures 1 and 2. These spectra were recorded by focus on the laser spots on the surfaces of as-grown PANI films. These films were obtained by scan voltammetrically for different cycles. The spectrum recorded at higher cycles reflects the spectral information of the thicker film. As we can see from the two figures, the Raman spectroscopic features of PANI depend strongly on the wavelength of the laser beam used for excitation. The Raman bands in the fingerprint region (<1000 cm^{-1}) are fairly low in the spectra obtained by excitation with the 633-nm laser beam. This indicates that the 785-nm laser beam is a more suitable laser to study the doping level of PANI. As has been reported in many previous articles, the enhancement of Raman modes is directly correlated to the UV-vis absorption. The absorbance of undoped PANI exhibits a very strong visible absorption band with a maximum located at about 630 nm, which was related to the quiniod structure of PANI.[10] However, the doped species only show a very weak absorption in this region. Therefore, when excited at 633 nm, the resonance effect selectively enhances the Raman bands associated with the quiniod structure. However, the polarons of doped PANI films have a broad electronic absorption band with a maximum about 950 nm.[11] In this region, the undoped species show a very weak absorption. The wavelength of the 785-nm laser beam is nearly in the middle between 630 and 950 nm. Neither the undoped nor the doped species show strong absorption

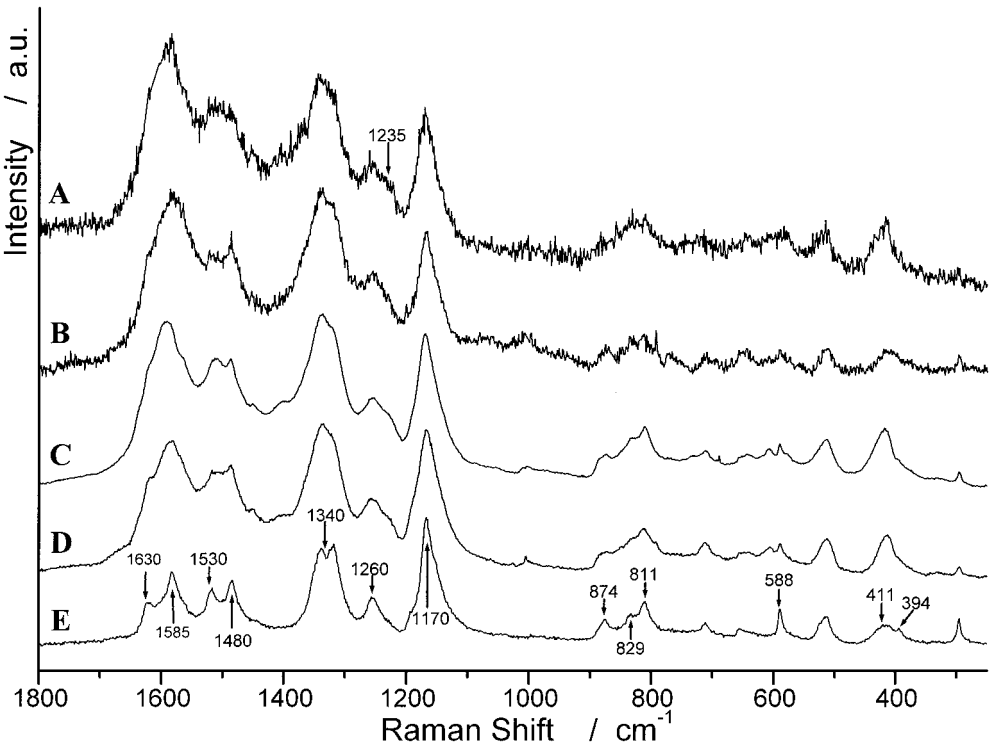

Figure 2 Excited Raman spectra, 633 nm, of PANI films deposited on Pt electrodes prepared by voltammetic scanning for different cycles in the potential scale between −0.2 and +0.75 V (versus SCE) at a potential scan rate of 0.02 V s^{-1}: (A) 30 cycles; (B) 50 cycles; (C) 80 cycles; (D) 100 cycles; (E) 120 cycles.

at this point. Therefore, the selective enhancement of the Raman bands related to the undoped or doped species can be greatly avoided. As a result, 785-nm laser-excited Raman spectra can give the structural information of undoped and doped species simultaneously. Moreover, it can be seen from the two figures that the features of the Raman spectra change dramatically with an increasing thickness of the PANI films. These variations also can be observed in Figure 3, which presents the changes of Raman spectra with the film thickness more distinctly.

Figure 3 shows 785-nm laser-excited Raman spectra of PANI film at different sampling depths using the microscopic confocal technique. The PANI film is obtained after a scan voltammetrically for 120 rounds under the experimental conditions mentioned above. The thickness of the sample is about 22 μm, measured by SEM graphs. The spectrum recorded at a higher laser confocal depth reflected the spectral information of the thinner film. The assignments of the Raman bands are listed in Table I.[12–18]

As can be seen from Figure 3, the overall features of the Raman spectra change dramatically with an increasing thickness of the PANI film, that is, the decrease of the laser confocal depth. Based on band separation (Fig. 4), the relative intensity of a single band can be read out. Accordingly, all the Raman bands associated with phenyl units are increased, while the bands related to quiniod units are decreased with increase of the film thickness. Moreover, the Raman bands of the semiquiniod cation increase gradually. The increased Raman bands of phenyl units are listed as follows: C—C stretching peak about 1610 cm^{-1}, C—C stretching peak about 1550 cm^{-1}, C—N stretching peak about 1260 cm^{-1}, C—H bending peak about 1185 cm^{-1} in-plane ring deformation peak about 874 cm^{-1}, out-plane ring deformation peak about 710 cm^{-1}, in-plane amine deformation peak about 588 cm^{-1}, and in-plane ring deformation peak about 394 cm^{-1}. The decreased Raman bands of quiniod units include the following: C═C stretching peak about 1590 cm^{-1} C═N stretching peak about 1490 cm^{-1}, in-plane ring deformation peak about 1235 cm^{-1}, in-plane ring deformation peak about 829 cm^{-1}, and imine deformation peak about 740 cm^{-1}. The variation tendencies of these peaks are listed in Table II. The Raman spectra results described above demonstrate that the doping level of PANI films increases with film thickening, because the quiniod structure converts to a semiquiniod structure during the doping process.

On the other hand, the Raman band centered about 811 cm^{-1}, assigned to the out-plane C—H deformation of the quiniod structure, increases when the film becomes thicker. This is because that, with the increasing of the film thickness, the film becomes rougher

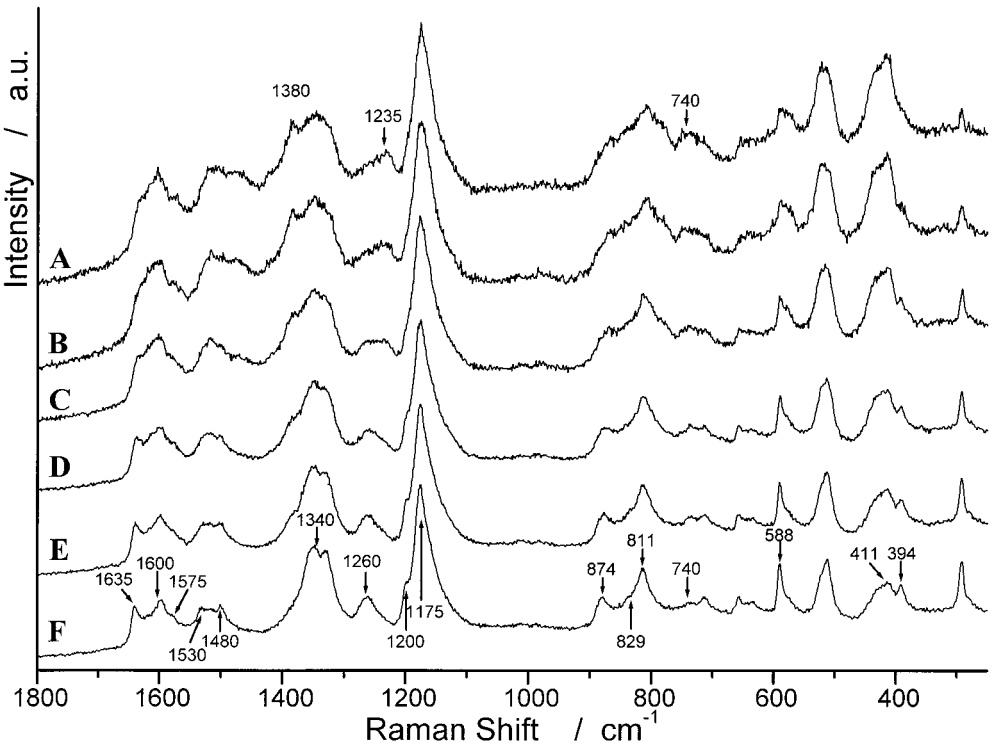

Figure 3 Laser-excited Raman spectra, 785 nm, of a PANI film deposited on Pt electrodes at different confocal depths using the microscopic confocal technique: (A) 20 μm; (B) 16 μm; (C) 12 μm; (D) 8 μm; (E) 4 μm; (F) 0 μm.

TABLE I
Band Assignments of the Raman Spectra of PANI Film

Wavenumber (cm^{-1})	Assignments
~1638	Cyclized structure containing nitrogen formed by crosslinking
1610–1600	B C—C stretching
1590–1575	Q C═C stretching
1550–1530	B C—C stretching
1510–1500	N—H bending
1490–1480	Q C═N stretching
1340–1330	SQR C—$N^{+\cdot}$ stretching
1260–1250	B C—N stretching
1235–1225	Q In-plane ring deformation
1200–1185	B In-plane C–H bending
1175–1165	Q In-plane C–H bending
~1121	In-plane C—H bending
~874	B In-plane ring deformation
~829	Q In-plane ring deformation
~811	Q Out-plane C—H deformation
~740	Q Imine deformation
~710	B Out-plane ring deformation
~679	Q Out-plane ring deformation
~640	B In-plane ring deformation
~588	B In-plane amine deformation
~556	Q In-plane ring deformation
~513	Out-plane C—N—C torsion
~411	Q Out-plane C–H wag
~394	B In-plane ring deformation

and the free volume of the polymer chain in the film increases, which leads to a relative out-plane vibration increase. This point was also confirmed by SEM.

Moreover, the Raman bands, centered about 1635 cm^{-1}, are also enhanced greatly with increase of the film thickness. This band is assigned to the cyclized structure containing nitrogen formed by the crosslinking of doped PANI,[19] and the increase of this band indicated that the crosslinking degree increases when the film becomes thicker.

An interesting Raman band is found about 1380 cm^{-1}, which was not identified clearly in previous publications.[19–21] This band decreases with increase of the PANI film thickness. Our experimental results indicate that this band disappears at a very high doping level. This phenomenon is identical with that of Cochet et al., who found that this band is observed only for PANI film with an intermediate doping level.[13]

The doping level increase of the PANI film during its electrochemical growth process also can be confirmed by XPS analysis. Usually, the doping level variation tendency of PANI can be demonstrated by the change of the atom number ratio of chlorine to nitrogen (Cl/N) or six times of that of chlorine to carbon (6Cl/C; six chlorine atoms correspond to one carbon atom in PANI doped with HCl).[22] However, the deviation of the nitrogen content resulting from nitrogen in the atmosphere cannot be neglected in the course of the sample analysis, even under a vacuum

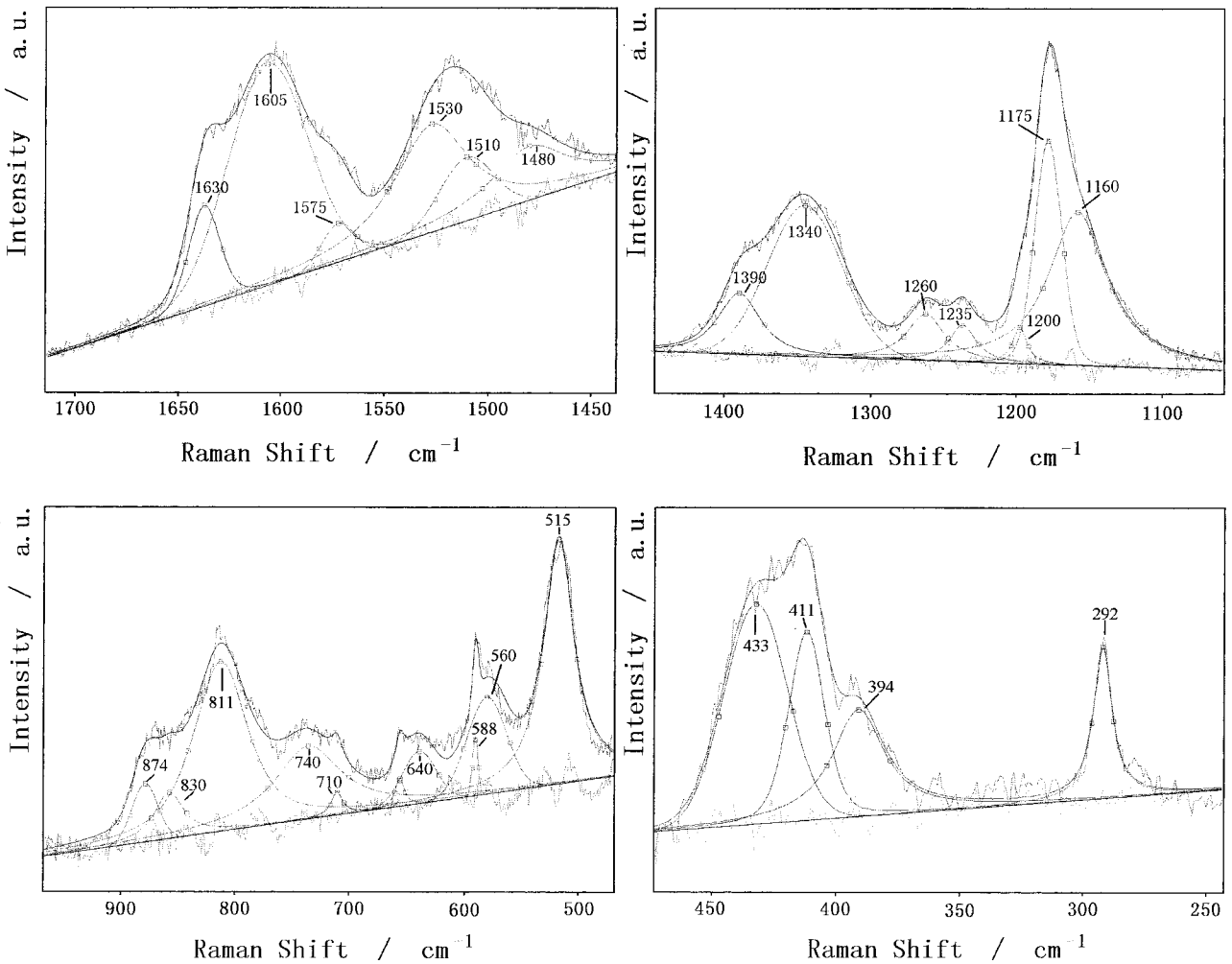

Figure 4 Typical sketch maps of Raman band separation.

condition. Moreover, nitrogen absorption may have occurred on the surface of the sample. Therefore, we chose a 6Cl/C ratio variation to indicate the doping level change of the PANI films. Table III lists the results of the 6Cl/C ratios of the PANI films. It can be seen from the table that the 6Cl/C ratios increase gradually with an increasing thickness of the PANI film, that is, the doping level of PANI film increases with the film thickness. It should be noted that XPS can provide only semiquantitative information of the components in the sample due to lack of a criterion. Therefore, the 6Cl/C ratios can only be used to estimate the doping level of PANI samples.

The doping process of PANI leads to a change of the UV-visible (UV) absorption spectrum. Therefore, the change of doping levels of PANI films can also be

TABLE II
Relative Raman Band Intensities Derived from the Raman Spectra of a PANI Sample Recorded at Different Confocal Depths

	Confocal depths (μm)					
Intensities	0	4	8	12	16	20
I_{1575}/I_{1605}	0.013	0.045	0.10	0.17	0.40	0.43
I_{1480}/I_{1530}	~0.0	0.031	0.20	0.50	0.99	1.0
I_{1340}/I_{1260}	2.8	2.9	2.7	3.2	4.0	5.0
I_{1235}/I_{1260}	0.14	0.25	0.29	0.79	1.8	2.0
I_{1175}/I_{1200}	3.2	3.5	4.4	6.1	13	19
I_{829}/I_{874}	0.36	0.57	0.34	0.79	1.2	1.6
I_{740}/I_{588}	0.26	0.38	0.65	1.2	5.2	4.9
I_{411}/I_{394}	1.0	1.2	1.6	1.8	3.0	3.8

TABLE III
Doping Level of PANI Film Indicated by 6Cl/C Ratios in Terms of PANI Film Grown Voltammetrically for Different Cycles

CV cycle number	6Cl/C ratio (%)
50	10.7
100	14.2
120	20.4

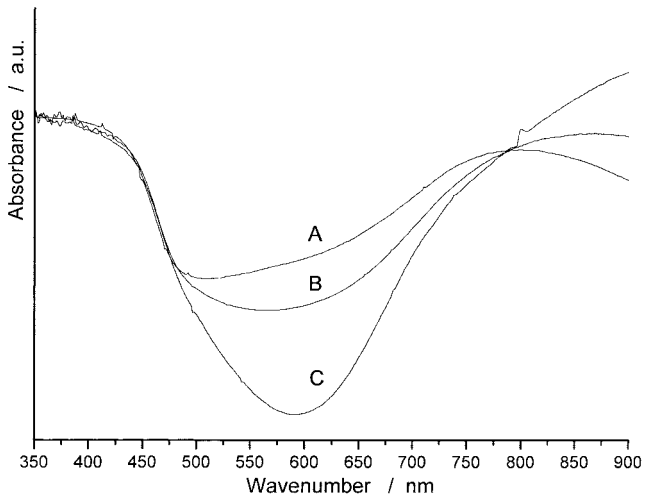

Figure 5 UV absorption of PANI film with different thicknesses deposited on ITO glass electrodes: (A) about 3.5 μm; (B) about 4.5 μm; (C) about 7.0 μm.

indicated by their UV absorption spectra. The typical UV absorption spectrum of PANI doped with HCl at different levels exhibits three absorption bands at the 300–1000 region, which is located about 325, 630, and 950 nm.[11,23] The absorptions at 325 and 630 nm are related to the excitation of benzene united and the quinoid ring, respectively, while the 950-nm band is attributed to the polarons which form by the doping of PANI. Previous research showed that, with increase of the doping level, the absorption at 630 nm decreases while that of the 950-nm bands increases. Figure 5 shows the UV absorption of PANI film with different thicknesses grown on ITO glass electrodes. The thickness of the polymer films was controlled by the electropolymerization time and were measured to be about 3.5 (A), 4.5 (B), and 7.0μm (C). It can be seen from Figure 5 that, with increase of the polymer film thickness, the absorption at 630 nm decreases gradually while that at 950 nm (limited to 900 nm) increases, although UV absorbance only gives the average information of doped PANI. These results indicate that the doping level of PANI increases with increase of the film thickness.

Why does the doping level of a compact PANI film increase during its electrochemical growth process? Our previous research demonstrated that the doping of a conducting polymer is a successive step of polymer formation and the film growth is a step faster than that of film doping. At the beginning, a smooth and compact PANI film was formed on the electrode surface through a two-dimensional growth process.[24] Therefore, it is difficult for the counterions (here is Cl^-) accompanied by solvent molecules in the electrolyte to insert into the film because of a lack of free volume in the film. This leads to the formation of lowly doped PANI. After the initial stage, the PANI deposition was gradually governed by three-dimensional nucleation under a charge-control mechanism.[24] The film becomes rougher and more porous as the film grows thicker. As a result, the diffusion of counterions into the film becomes easier and easier and the doping level of the film increases. The morphology variation of PANI during the growth process is shown in Figure 6. Similar phenomena have been observed on polypyrrole and polythiophene films electrochemically deposited from acetonitrile or boron trifluoride diethyl etherate (BFEE) solutions.

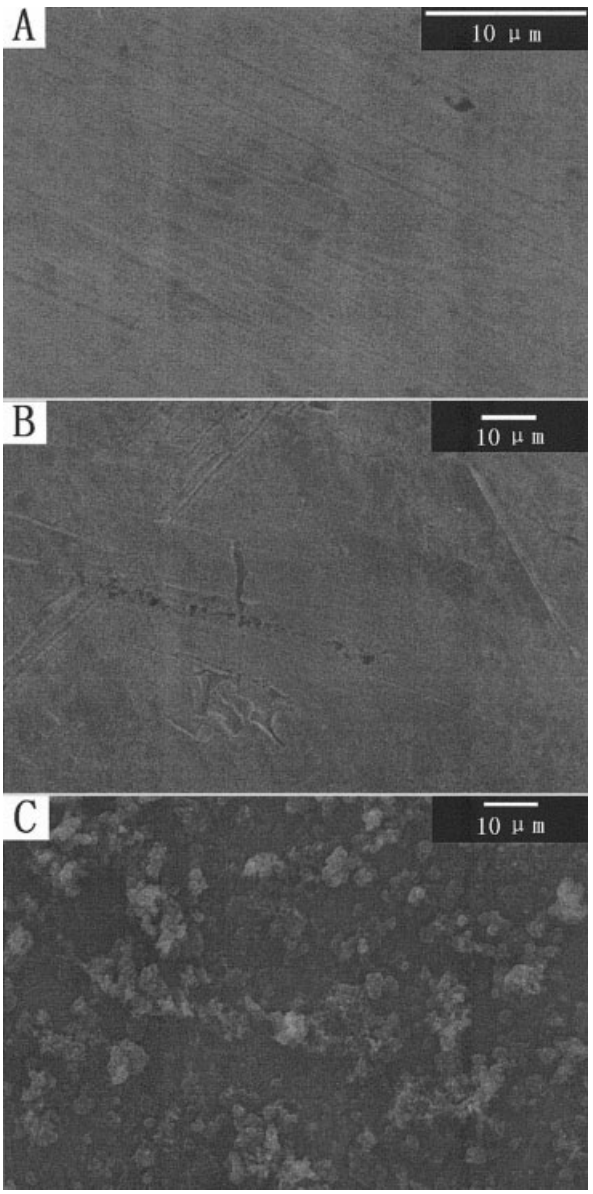

Figure 6 SEMs of PANI films deposited on Pt electrodes with different growth cycles in the potential scale between -0.2 and $+0.75$ V (versus SCE) at a potential scan rate of 0.02 V s^{-1}: (A) 30 cycles; (B) 80 cycles; (C) 120 cycles.

CONCLUSIONS

The doping level of electrochemically deposited PANI films increases with increase of the film thickness. This finding was confirmed using Raman, XPS, and UV-visible spectroscopies. During the electrochemical polymerization process, a smooth and compact PANI film was formed on the electrode initially. Thus, the counterions cannot diffuse into the film and lead to a lowly doped film. The morphology of the polymer film becomes more porous and irregular as the film thickens. This results in easier ion diffusion and higher doping levels of the films.

This work was supported by the National Natural Science Foundation of China (Grant Numbers 50133010, 20374034, and 50225311).

References

1. Green, A. G.; Woodhead, A. E. J Chem Soc Trans 1910, 97, 2388; 1912, 101, 1117.
2. Kang, E. T.; Neoh, K. G.; Tan, K. L. Prog Polym Sci 1998, 23, 277.
3. de Oliveira, Z. T., Jr.; dos Santos, M. C. Chem Phys 2000, 260, 95.
4. Zeng, X.; Ko, T. M. Polymer 1998, 39, 1187.
5. Majidi, M. R.; Kane-Maguire, L. A. P.; Wallace, G. G. Polymer 1994, 14, 3113.
6. Fu, M.; Shi, G.; Chen F.; Hong, X. Phys Chem Chem Phys 2002, 4, 2685.
7. Xu, J.; Shi, G.; Chen, F.; Hong, X. Chin Polym Sci 2002, 20, 425.
8. Chen, F.; Shi, G.; Fu, M.; Qu, L.; Hong, X. Synth Met 2003, 132, 125.
9. Cheng, N.; Hu, S. Handbook of Solvents; Chemical Engineering: Beijing, 1986.
10. Masters, J. G.; Ginder, J. M.; MacDiarmid, A. G.; Epstein, A. J. J Chem Phys 1992, 96, 4768.
11. Wan, M. J Polym Sci Part A Polym Chem 1992, 30, 543.
12. Cochet, M.; Louarn, G.; Quillard, S.; Boyer, M. I.; Buisson, J. P.; Lefrant, S. J Raman Spectrosc 2000, 31, 1029.
13. Cochet, M.; Louarn, G.; Quillard, S.; Buisson, J. P.; Lefrant, S. J Raman Spectrosc 2000, 31, 1041.
14. Quillard, S.; Louarn, G.; Lefrant, S.; MacDiarmid, A. G. Phys Rev 1994, 17, 12496.
15. Lindfors, T.; Kvarnström, C.; Ivaska, A. J Electroanal Chem 2002, 518, 131.
16. Louarn, G.; Lapkowski, M.; Quillard, S.; Pron, A.; Buisson, J. P.; Lefrant, S. J Phys Chem 1996, 100, 6998.
17. Berrada, K.; Quillard, S.; Louarn, G.; Lefrant, S. Synth Met 1995, 69, 201.
18. Furukawa, Y.; Ueda, F.; Hyodo, Y.; Harada, I.; Nakajima, T.; Kawagoe, T. Macromolecules 1988, 21, 1297.
19. Pereira da Silva, J. E.; de Faria, D. L. A.; Córdoba de Torresi, S. I.; Temperini, M. L. A. Macromolecules 2000, 33, 3077.
20. Pereira da Silva, J. E.; Córdoba de Torresi, S. I.; de Faria, D. L. A.; Temperini. M. L. A. Synth Met 1999, 101, 834.
21. Pereira da Silva, J. E.; Temperini, M. L. A.; Córdoba de Torresi, S. I. Electrochim Acta 1999, 44, 1887.
22. MacDiarmid, A. G.; Chiang, J. C.; Richter, A. F.; Somasiri N. L. D.; Epstein, A. J. In Conducting Polymers; Alcacer, L., Ed.; Reidel: Dordrecht, 1987.
23. MacDiarmid, A. G.; Epstein, A. J. Synth Met 1994, 65, 103.
24. Villareal, I.; Morales, E.; Acosta, J. L. Polymer 2001, 42, 3779.